Paper 287

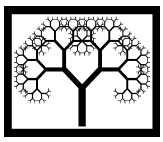

Proceedings of the Tenth International Conference
on Computational Structures Technology,
B.H.V. Topping, J.M. Adam, F.J. Pallarés,
R. Bru and M.L. Romero, (Editors),
Civil-Comp Press, Stirlingshire, Scotland

A Higher-Order Exact Geometry Solid-Shell Element undergoing Finite Rotations

S.V. Plotnikova and G.M. Kulikov
Department of Applied Mathematics and Mechanics
Tambov State Technical University, Russia

Abstract

This paper presents the non-linear exact geometry assumed stress-strain four-node element with nine displacement degrees of freedom per node. The finite element formulation developed is based on the 9-parameter shell model by employing a new concept of interpolation surfaces (I-surfaces) inside the shell body. We introduce three I-surfaces and choose nine displacements of these surfaces as fundamental shell unknowns. Such choice allows us to represent the finite rotation higher-order shell formulation in a very compact form and to derive in curvilinear reference surface coordinates the strain-displacement relationships, which are objective, that is, invariant under large rigid-body motions.

Keywords: nine-parameter shell model, finite rotation, exact geometry solid-shell element.

1 Introduction

A large number of works has been already done to develop the finite rotation higher-order shell formulation with thickness stretching. These works are devoted as a rule to the 7-parameter shell theory [1, 2] in which the transverse normal strain varies at least linearly through the shell thickness. This fact is of great importance since the popular 6-parameter shell formulation [3, 4] based on the complete 3D constitutive equations exhibits thickness locking. The errors caused by thickness locking do not decrease with the mesh refinement because the reason of stiffening lies in the shell theory itself rather than the finite element discretization.

It is well-known that a conventional way for developing the higher-order shell formulation is to utilize either quadratic or cubic series expansions in the thickness coordinate and to choose as unknowns the generalized displacements of the midsurface. Herein, the 9-parameter shell model is developed using a new concept of interpolation surfaces (I-surfaces) inside the shell body [5]. The I-surfaces are introduced

in order to choose the values of displacements with correspondence to these surfaces as fundamental unknowns. Taking into account that displacement vectors of I-surfaces are resolved in the reference surface frame the proposed higher-order shell formulation is very promising for developing high performance exact geometry solid-shell elements.

2 Kinematic Description of Undeformed Shell

Let us consider a shell of the thickness h. The shell can be defined as a 3D body of volume V bounded by two outer surfaces Ω^- and Ω^+, located at the distances d^- and d^+ measured with respect to the reference surface Ω such that $h = d^- + d^+$, and the edge boundary surface Σ. The reference surface is assumed to be sufficiently smooth and without any singularities. As has been shown recently [4], this assumption cannot introduce any serious limitation in the shell theory because in the case of the robust choice of the reference surface we are able to model general surface geometry such as shell intersections and shell edges efficiently. Let the reference surface be referred to the convected curvilinear coordinates θ^1 and θ^2, whereas the coordinate θ^3 is oriented along the unit vector $\boldsymbol{a}_3 = \boldsymbol{a}^3$ normal to the reference surface. As I-surfaces, we choose the bottom and top surfaces and the midsurface Ω^{M} as well [2, 5].

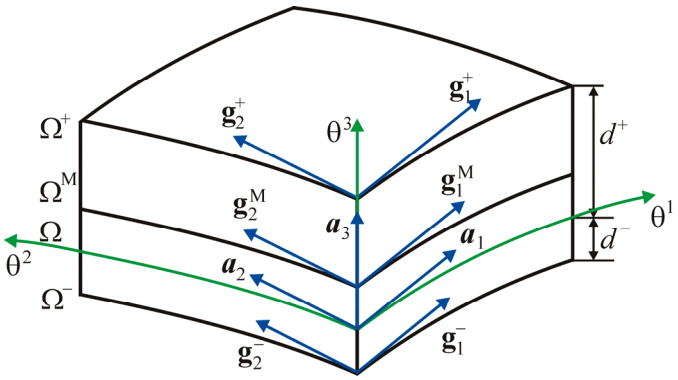

Figure 1: Geometry of the shell

Introduce in accordance with Figures 1 and 2 the following notations: $\mathbf{r} = \mathbf{r}\left(\theta^1, \theta^2\right)$ is the position vector of any point of the reference surface; $\boldsymbol{a}_\alpha = \mathbf{r}_{,\alpha}$ are the covariant base vectors of the reference surface; $\boldsymbol{a}^\beta$ are the contravariant base vectors of the reference surface defined by the standard relation $\boldsymbol{a}_\alpha \cdot \boldsymbol{a}^\beta = \delta_\alpha^\beta$; $a_{\alpha\beta} = \boldsymbol{a}_\alpha \cdot \boldsymbol{a}_\beta$ and $a^{\alpha\beta} = \boldsymbol{a}^\alpha \cdot \boldsymbol{a}^\beta$ are the covariant and contravariant components of the metric tensor of the reference surface; $a = \det\left[a_{\alpha\beta}\right]$ is the determinant of the metric tensor of the reference surface; b_α^β are the mixed components of the curva-

ture tensor defined as

$$b_\alpha^\beta = -\boldsymbol{a}^\beta \cdot \boldsymbol{a}_{3,\alpha}; \tag{1}$$

$\mathbf{R}$ is the position vector of any point in the shell body given by

$$\mathbf{R} = \mathbf{r} + \theta^3 \boldsymbol{a}_3; \tag{2}$$

in particular, position vectors of I-surfaces are

$$\mathbf{R}^I = \mathbf{r} + z^I \boldsymbol{a}_3, \tag{3}$$

where z^I are the transverse coordinates of I-surfaces defined as

$$z^- = -d^-, \quad z^+ = d^+, \quad z^{\mathrm{M}} = \frac{1}{2}\left(z^- + z^+\right); \tag{4}$$

μ_α^β are the mixed components of the 3D shifter tensor expressed as

$$\mu_\alpha^\beta = \delta_\alpha^\beta - \theta^3 b_\alpha^\beta; \tag{5}$$

in particular, components of the shifter tensor at I-surfaces are

$$\mu_\alpha^{I\beta} = \delta_\alpha^\beta - z^I b_\alpha^\beta; \tag{6}$$

$\mathbf{g}_i$ are the covariant base vectors in the shell body defined as

$$\mathbf{g}_\alpha = \mathbf{R}_{,\alpha} = \mu_\alpha^\beta \boldsymbol{a}_\beta, \quad \mathbf{g}_3 = \mathbf{R}_{,3} = \boldsymbol{a}_3; \tag{7}$$

in particular, base vectors of I-surfaces are

$$\mathbf{g}_\alpha^I = \mathbf{R}_{,\alpha}^I = \mu_\alpha^{I\beta} \boldsymbol{a}_\beta, \quad \mathbf{g}_3^I = \boldsymbol{a}_3; \tag{8}$$

g_{ij} are the covariant components of the 3D metric tensor given by

$$g_{\alpha\beta} = \mathbf{g}_\alpha \cdot \mathbf{g}_\beta = \mu_\alpha^\gamma \mu_\beta^\delta a_{\gamma\delta}, \quad g_{i3} = \mathbf{g}_i \cdot \mathbf{g}_3 = \delta_{i3}; \tag{9}$$

in particular, components of the metric tensors of I-surfaces are

$$g_{\alpha\beta}^I = \mathbf{g}_\alpha^I \cdot \mathbf{g}_\beta^I = \mu_\alpha^{I\gamma} \mu_\beta^{I\delta} a_{\gamma\delta}, \quad g_{i3}^I = \mathbf{g}_i^I \cdot \mathbf{g}_3^I = \delta_{i3}; \tag{10}$$

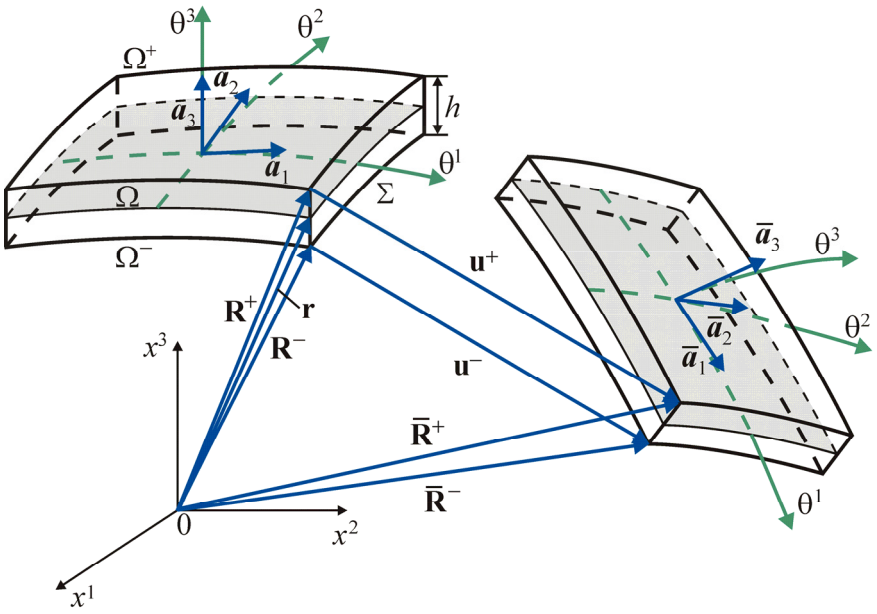

Figure 2: Initial and current configurations of the shell

$g = \det\left[g_{ij}\right]$ is the determinant of the 3D metric tensor; $g^I = \det\left[g^I_{ij}\right]$ are the determinants of the metric tensors of I-surfaces; $\mu = \sqrt{g/a}$ is the determinant of the shifter tensor; $\mu^I = \sqrt{g^I/a}$ are the determinants of the shifter tensor at I-surfaces; $(\ldots)_{,i}$ are the partial derivatives in V with respect to coordinates θ^i; $(\ldots)|_\alpha$ are the covariant derivatives in Ω with respect to coordinates θ^α. Here and in the following developments, Greek tensorial indices $\alpha, \beta, \gamma, \delta$ range from 1 to 2; Latin tensorial indices i, j, m, n range from 1 to 3; Greek indices A, B identify the belonging of any quantity to the bottom and top surfaces and take values $-$ and $+$; Latin indices *I, J* identify the belonging of any quantity to the I-surfaces and take values $-$, $+$ and M.

3 Kinematic Description of Deformed Shell

Now, we introduce the first assumption for the proposed shell theory.

Assumption 1. The displacement field is approximated in the thickness direction according to the quadratic law

$$\mathbf{u} = \sum_I L^I \mathbf{u}^I, \tag{11}$$

where $\mathbf{u}^I\left(\theta^1, \theta^2\right)$ are the displacement vectors of I-surfaces; $L^I\left(\theta^3\right)$ are the Lagrange polynomials of the second order expressed as

$$\begin{aligned} L^- &= \frac{2}{h^2}\left(z^{\mathrm{M}} - \theta^3\right)\left(z^+ - \theta^3\right), \\ L^{\mathrm{M}} &= \frac{4}{h^2}\left(\theta^3 - z^-\right)\left(z^+ - \theta^3\right), \\ L^+ &= \frac{2}{h^2}\left(\theta^3 - z^-\right)\left(\theta^3 - z^{\mathrm{M}}\right), \end{aligned} \tag{12}$$

such that $L^I\left(z^J\right) = 1$ for $J = I$ and $L^I\left(z^J\right) = 0$ for $J \neq I$. Thus, we deal with the higher-order 9-parameter shell model because nine displacements of I-surfaces are introduced by Equation (11).

It is convenient to rewrite Equations (2) and (7) in more general forms

$$\mathbf{R} = \sum_I L^I \mathbf{R}^I, \qquad \mathbf{R}^{\mathrm{M}} = \frac{1}{2}\left(\mathbf{R}^- + \mathbf{R}^+\right) \tag{13}$$

and

$$\begin{aligned} \mathbf{g}_\alpha &= \sum_I L^I \mathbf{g}^I_\alpha, \qquad \mathbf{g}^{\mathrm{M}}_\alpha = \frac{1}{2}\left(\mathbf{g}^-_\alpha + \mathbf{g}^+_\alpha\right), \\ \mathbf{g}_3 &= \sum_A N^A \mathbf{g}^A_3, \qquad \mathbf{g}^A_3 = \boldsymbol{a}_3, \end{aligned} \tag{14}$$

where $N^A\left(\theta^3\right)$ are the polynomials of the first order defined as

$$N^- = \frac{1}{h}\left(z^+ - \theta^3\right), \quad N^+ = \frac{1}{h}\left(\theta^3 - z^-\right), \tag{15}$$

such that $N^A\left(z^B\right) = 1$ for $B = A$ and $N^A\left(z^B\right) = 0$ for $B \neq A$.

Using Equations (11) and (13), we arrive at the formula for the position vector of the deformed shell

$$\overline{\mathbf{R}} = \mathbf{R} + \mathbf{u} = \sum_I L^I \overline{\mathbf{R}}^I, \tag{16}$$

where $\overline{\mathbf{R}}^I\left(\theta^1, \theta^2\right)$ are the position vectors of I-surfaces given by

$$\overline{\mathbf{R}}^I = \mathbf{R}^I + \mathbf{u}^I. \tag{17}$$

The covariant base vectors in the current shell configuration are

$$\overline{\mathbf{g}}_\alpha = \overline{\mathbf{R}}_{,\alpha} = \sum_I L^I \overline{\mathbf{g}}_\alpha^I, \tag{18}$$

$$\overline{\mathbf{g}}_3 = \overline{\mathbf{R}}_{,3} = \sum_A N^A \overline{\mathbf{g}}_3^A.$$

Here, $\overline{\mathbf{g}}_\alpha^I$ and $\overline{\mathbf{g}}_3^A$ are the base vectors of I-surfaces of the deformed shell expressed as

$$\overline{\mathbf{g}}_\alpha^I = \overline{\mathbf{R}}_{,\alpha}^I = \mathbf{g}_\alpha^I + \mathbf{u}_{,\alpha}^I, \quad \mathbf{g}_3^A = \boldsymbol{a}_3 + \boldsymbol{\beta}^A, \tag{19}$$

where

$$\boldsymbol{\beta}^A = \mathbf{u}_{,3}\left(z^A\right), \tag{20}$$

that can be represented by using Equations (11) and (12) as follows:

$$\boldsymbol{\beta}^- = \frac{1}{h}\left(-3\mathbf{u}^- + 4\mathbf{u}^{\mathrm{M}} - \mathbf{u}^+\right), \quad \boldsymbol{\beta}^+ = \frac{1}{h}\left(\mathbf{u}^- - 4\mathbf{u}^{\mathrm{M}} + 3\mathbf{u}^+\right). \tag{20a}$$

4 Strain-Displacement Relationships

The Green-Lagrange strain tensor can be written as

$$2\varepsilon_{ij} = \overline{\mathbf{g}}_i \cdot \overline{\mathbf{g}}_j - \mathbf{g}_i \cdot \mathbf{g}_j. \tag{21}$$

Substituting base vectors (14) and (18) into relationships (21), one finds

$$2\varepsilon_{\alpha\beta} = \sum_{I,J} L^I L^J \left(\mathbf{u}_{,\alpha}^I \cdot \mathbf{g}_\beta^J + \mathbf{u}_{,\beta}^J \cdot \mathbf{g}_\alpha^I + \mathbf{u}_{,\alpha}^I \cdot \mathbf{u}_{,\beta}^J\right), \tag{22}$$

$$2\varepsilon_{\alpha 3} = \sum_{A,I} N^A L^I \left(\mathbf{u}_{,\alpha}^I \cdot \boldsymbol{a}_3 + \boldsymbol{\beta}^A \cdot \mathbf{g}_\alpha^I + \boldsymbol{\beta}^A \cdot \mathbf{u}_{,\alpha}^I\right),$$

$$2\varepsilon_{33} = \sum_{A,B} N^A N^B \left(\boldsymbol{\beta}^A \cdot \boldsymbol{a}_3 + \boldsymbol{\beta}^B \cdot \boldsymbol{a}_3 + \boldsymbol{\beta}^A \cdot \boldsymbol{\beta}^B\right).$$

It is seen from Equations (12), (15) and (22) that in-plane strains $\varepsilon_{\alpha\beta}$ are the polynomials of the fourth order, transverse shear strains $\varepsilon_{\alpha 3}$ are the polynomials of the third order and a transverse normal strain ε_{33} is the polynomial of the second order. To simplify the higher-order 9-parameter shell formulation, we introduce the next assumption.

Assumption 2. From the mechanical point of view it is convenient to assume that all components of the Green-Lagrange strain tensor are distributed through the thickness of the shell according to the displacement distribution (11), i.e.,

$$\breve{\varepsilon}_{ij} = \sum_I L^I \varepsilon_{ij}^I, \tag{23}$$

where $\varepsilon_{ij}^I = \varepsilon_{ij}\left(z^I\right)$ are the *exact values* of Green-Lagrange strains at I-surfaces defined as

$$\begin{gathered} 2\varepsilon_{\alpha\beta}^I = \mathbf{u}_{,\alpha}^I \cdot \mathbf{g}_\beta^I + \mathbf{u}_{,\beta}^I \cdot \mathbf{g}_\alpha^I + \mathbf{u}_{,\alpha}^I \cdot \mathbf{u}_{,\beta}^I, \\ 2\varepsilon_{\alpha 3}^I = \mathbf{u}_{,\alpha}^I \cdot \boldsymbol{a}_3 + \boldsymbol{\beta}^I \cdot \mathbf{g}_\alpha^I + \boldsymbol{\beta}^I \cdot \mathbf{u}_{,\alpha}^I, \\ 2\varepsilon_{33}^I = 2\boldsymbol{\beta}^I \cdot \boldsymbol{a}_3 + \boldsymbol{\beta}^I \cdot \boldsymbol{\beta}^I. \end{gathered} \tag{24}$$

Here, an additional notation has been introduced

$$\boldsymbol{\beta}^{\mathrm{M}} = \mathbf{u}_{,3}\left(z^{\mathrm{M}}\right) = \frac{1}{h}\left(\mathbf{u}^+ - \mathbf{u}^-\right). \tag{25}$$

Actually, this assumption implies that now all strain components $\breve{\varepsilon}_{ij}$ are the polynomials of the second order that simplifies sufficiently the non-linear higher-order 9-parameter shell formulation.

Remark 1. It can be verified by using Equations (12) and (15) that components of the simplified and exact Green-Lagrange strain tensors satisfy linking conditions

$$\breve{\varepsilon}_{ij}\left(z^I\right) = \varepsilon_{ij}\left(z^I\right) = \varepsilon_{ij}^I. \tag{26}$$

These links are illustrated by means of Figure 3. It should be also noticed that the non-uniform distribution of the transverse normal strain in the thickness direction permits to utilize 3D constitutive laws. In principle, the linear strain distribution is sufficient for this purpose [1].

We next represent displacement vectors of I-surfaces as follows:

$$\mathbf{u}^I = u_i^I \boldsymbol{a}^i. \tag{27}$$

It is seen that displacement vectors are resolved in the contravariant reference surface basis $\boldsymbol{a}^i$ that allows us to reduce the costly numerical integration by evaluating the stiffness matrix [2-4]. The derivatives of displacement vectors $\boldsymbol{\beta}^I$ from Equations (20) and (25) can be represented in a similar way

$$\boldsymbol{\beta}^I = \beta_i^I \boldsymbol{a}^i, \tag{28}$$

$$\beta_i^- = \frac{1}{h}\left(-3u_i^- + 4u_i^{\mathrm{M}} - u_i^+\right),\ \beta_i^+ = \frac{1}{h}\left(u_i^- - 4u_i^{\mathrm{M}} + 3u_i^+\right),$$

$$\beta_i^{\mathrm{M}} = \frac{1}{h}\left(u_i^+ - u_i^-\right).$$

The derivatives of displacement vectors of I-surfaces are written as

$$\mathbf{u}_{,\alpha}^I = u_i^I\ |_\alpha\ \boldsymbol{a}^i, \tag{29}$$

$$u_i^I\ |_\alpha = u_{i,\alpha}^I - \Gamma_{i\alpha}^j u_j^I, \tag{30}$$

where $\Gamma_{i\alpha}^{j}$ are the Christoffel symbols defined as

$$\Gamma_{\alpha\beta}^{i} = \boldsymbol{a}^{i} \cdot \boldsymbol{a}_{\alpha,\beta}, \qquad \Gamma_{3\alpha}^{\beta} = -b_{\alpha}^{\beta}, \qquad \Gamma_{3\alpha}^{3} = 0. \tag{31}$$

Substituting Equations (8), (28) and (29) into strain-displacement relationships (24), we arrive at a scalar form of these relationships

$$\begin{aligned} 2\varepsilon_{\alpha\beta}^{I} &= \mu_{\beta}^{I\gamma} u_{\gamma}^{I} \mid_{\alpha} + \mu_{\alpha}^{I\gamma} u_{\gamma}^{I} \mid_{\beta} + a^{ij} u_{i}^{I} \mid_{\alpha} u_{j}^{I} \mid_{\beta}, \\ 2\varepsilon_{\alpha 3}^{I} &= u_{3}^{I} \mid_{\alpha} + \mu_{\alpha}^{I\gamma} \beta_{\gamma}^{I} + a^{ij} \beta_{i}^{I} u_{j}^{I} \mid_{\alpha}, \\ 2\varepsilon_{33}^{I} &= 2\beta_{3}^{I} + a^{ij} \beta_{i}^{I} \beta_{j}^{I}, \end{aligned} \tag{32}$$

where for convenience an additional notation $a^{i3} = \delta^{i3}$ has been introduced.

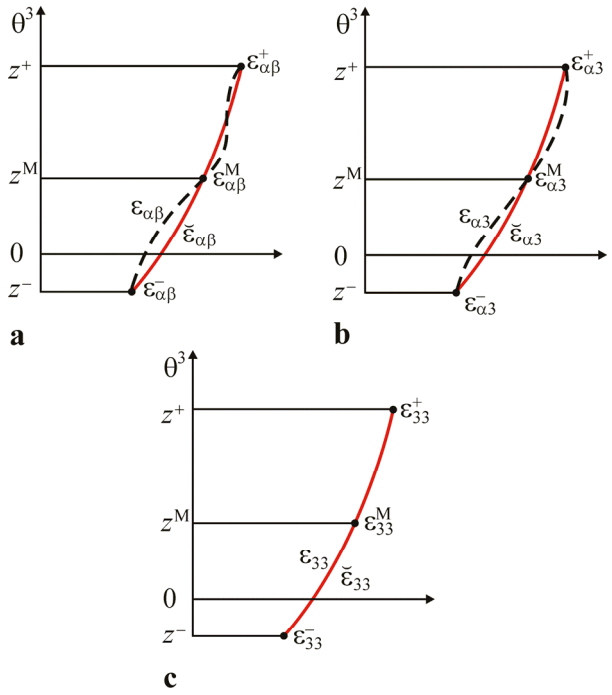

Figure 3: Approximate (——) and exact (– –) distributions of (a) in-plane, (b) transverse shear and (c) transverse normal strains through the thickness of the shell for the higher-order 9-parameter shell theory

We now formulate the fundamental statement concerning the Green-Lagrange strain tensor developed.

Proposition 1. The Green-Lagrange strain components (23) are objective, that is, they represent precisely large rigid-body shell motions in any convected curvilinear coordinate system.

Proof. The large rigid-body shell displacements can be defined as

$$(\mathbf{u})^{\text{Rigid}} = \boldsymbol{\Delta} + \boldsymbol{\Phi}\mathbf{R} - \mathbf{R}, \tag{33}$$

where $\boldsymbol{\Delta} = \Delta_{i}\boldsymbol{a}^{i}$ is the constant displacement (translation) vector; $\boldsymbol{\Phi}$ is the orthogonal rotation matrix [3]. In particular, rigid-body shell displacements of I-surfaces

are written as

$$\left(\mathbf{u}^I\right)^{\text{Rigid}} = \boldsymbol{\Delta} + \boldsymbol{\Phi}\mathbf{R}^I - \mathbf{R}^I. \tag{34}$$

The derivatives of the translation vector and the rotation matrix with respect to convected coordinates are zero, that is,

$$\boldsymbol{\Delta}_{,\alpha} = \mathbf{0} \quad \text{and} \quad \boldsymbol{\Phi}_{,\alpha} = \mathbf{0}. \tag{35}$$

Allowing for Equations (8) and (35), the derivatives of displacement vectors (34) are expressed as

$$\left(\mathbf{u}^I_{,\alpha}\right)^{\text{Rigid}} = \boldsymbol{\Phi}\mathbf{g}^I_\alpha - \mathbf{g}^I_\alpha. \tag{36}$$

Using Equations (20), (25) and (34), and taking into account formulas for the position vectors of I-surfaces (3) and (13) as well, one obtains

$$\left(\boldsymbol{\beta}^I\right)^{\text{Rigid}} = \boldsymbol{\Phi}\boldsymbol{a}_3 - \boldsymbol{a}_3. \tag{37}$$

It may be verified by employing Equations (36) and (37) that strains of I-surfaces (24) are all zero in a general large rigid-body shell motion:

$$2\left(\varepsilon^I_{ij}\right)^{\text{Rigid}} = \left(\boldsymbol{\Phi}\mathbf{g}^I_i\right)\cdot\left(\boldsymbol{\Phi}\mathbf{g}^I_j\right) - \mathbf{g}^I_i \cdot \mathbf{g}^I_j = 0. \tag{38}$$

This conclusion is true because the orthogonal transformation retains the scalar product of vectors. Therefore, due to Equation 38 the simplified Green-Lagrange strains (23) exactly represent arbitrarily large rigid-body motions, i.e.,

$$\left(\breve{\varepsilon}_{ij}\right)^{\text{Rigid}} = 0, \tag{39}$$

that completes the proof.

Thus, we have derived strain-displacement relationships (23) and (32) of the higher-order 9-parameter shell model, which exactly represent arbitrarily large rigid-body motions in a convected curvilinear coordinate system.

5 Finite element formulation

The proposed finite element formulation is based on a simple and efficient approximation of shells via exact geometry four-node solid-shell elements. The term "exact geometry" reflects the fact that coefficients of the first and second fundamental forms are taken exactly at every integration point. Therefore, no approximation of the reference surface is needed. To avoid shear and membrane locking and have no spurious zero energy modes, the assumed strain and stress resultant fields are introduced

$$\varepsilon^{\text{AS}}_{ij} = \sum_I L^I E^I_{ij}, \tag{40}$$

$$H^I_{ij} = \int_{z^-}^{z^+} L^I \sigma_{ij} d\theta^3, \tag{41}$$

where $E^I_{ij}\left(\theta^1,\theta^2\right)$ are the assumed strains of I-surfaces.

In this connection the Hu-Washizu variational principal has to be applied. Taking into account that displacement vectors of I-surfaces are represented in the reference

surface frame (27), the developed finite element formulation has computational advantages compared with conventional isoparametric hybrid/mixed formulations because our elemental stiffness matrix requires only direct substitutions, i.e., no matrix inversion is needed, and it is evaluated by using the full analytical integration [2, 6]. Note also that the finite element formulation is similar to the 7-parameter finite element formulation [2] and does not discussed here in detail.

6 Numerical Examples

The robustness of the proposed exact geometry four-node solid-shell element EG9P4 is assessed with several problems extracted from the literature. To substantiate this point we invoke high performance isoparametric elements and an exact geometry four-node solid-shell element EG6P4 [3, 6] based on the 6-parameter model.

6.1 Geometrically Linear Examples

6.1.1 Rectangular Homogeneous Plate

Consider first a rectangular homogeneous simply supported plate subjected to the sinusoidally distributed pressure load (Figure 4) with material data $E = 10^7$ and $\nu = 0.3$. Due to symmetry of the problem, only one quarter of the plate is modeled by 32×32 mesh of EG9P4 elements. A comparison with analytical solutions based on the elasticity theory [7] and classical plate theory (CPT) as well is given in Figure 5.

6.1.2 Rectangular Cross-Ply Plate

Next we study a rectangular two-layer cross-ply simply supported plate subjected to sinusoidal loading (Figure 4) with ply-orientation [0/90] and $E_L = 2.5 \times 10^7$, $E_T = 10^6$, $G_{LT} = 5 \times 10^5$, $G_{TT} = 2 \times 10^5$, $\nu_{LT} = \nu_{TT} = 0.25$. Due to symmetry, one quarter of the plate is discretized again by 32×32 mesh of EG9P4 elements. Figure 6 displays the transverse midsurface displacement at the center point and a comparison with analytical solutions based on the elasticity theory [8] and classical plate theory.

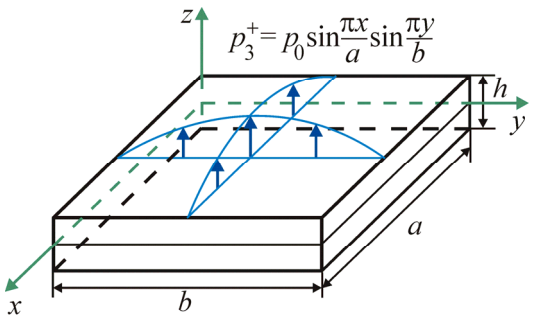

Figure 4: Rectangular plate $(a = b)$

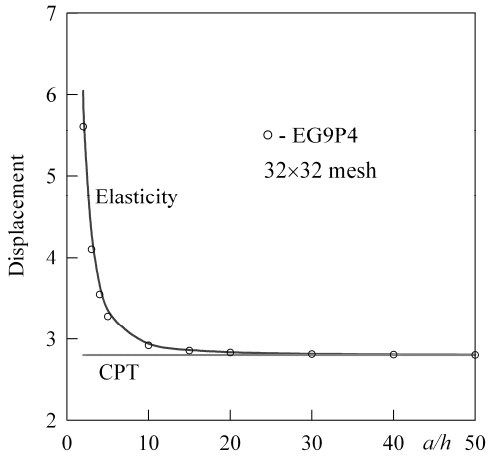

Figure 5: Transverse displacement at center point $100Eh^3u_{30}^{\mathrm{M}} / p_0a^4$ of the rectangular homogeneous plate

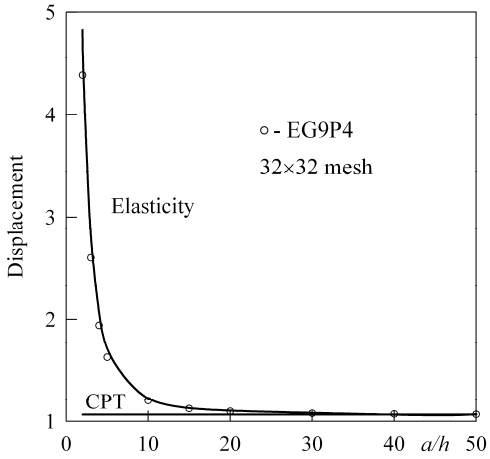

Figure 6: Transverse displacement at center point $100E_Th^3u_{30}^{\mathrm{M}} / p_0a^4$ of the rectangular two-layer cross-ply plate

6.1.3 Pinched Cylindrical Shell

To illustrate the capability of the developed exact geometry four-node solid-shell element to overcome membrane and shear locking phenomena and to compare it with high performance isoparametric four-node quadrilateral elements, we consider one of the most demanding standard linear tests, namely, a short cylindrical shell supported by two rigid diaphragms at the ends and loaded by two opposite concentrated forces in its middle section.

Owing to symmetry of the problem, only one octant of the shell is modeled with regular meshes of EG9P4 elements (Figure 7). Table 1 lists the normalized transverse displacement under the applied load and a comparison with isoparametric elements extracted from the literature in [6]. The displacement is normalized with respect to the well-known analytical solution -1.8248×10^{-5}. As can be seen, both

exact geometry shell elements exhibit an excellent performance for coarse meshes but the EG9P4 element is a bit stiff because of using the complete 3D constitutive equations.

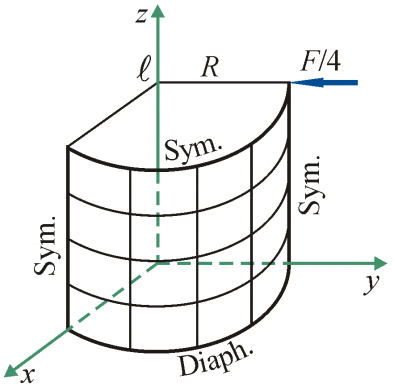

Figure 7: Pinched cylindrical shell with rigid diaphragms, where

$$R = 300,\ \ell = 300,\ h = 3,\ E = 3\times10^{6},\ \nu = 0.3,\ F = 1$$

Mesh	Isoparametric elements (see [6])			Exact geometry shell elements	
	Hughes, Liu	Bathe, Dvorkin	Simo et al.	EG6P4 [6]	EG9P4
4x4	0.373	0.370	0.399	0.8900	0.8691
8x8	0.747	0.740	0.763	0.9412	0.9322
16x16	0.935	0.930	0.935	0.9861	0.9826

Table 1: Normalized transverse displacement u_3^{M} under applied load of the pinched cylindrical shell

6.1.4 Cross-ply hyperbolic shell

A three-layer cross-ply hyperbolic shell subjected to two pairs of opposite concentrated forces was proposed for testing non-linear formulations for composite shells, while we employ this example as a linear benchmark test to assess the analytical integration schemes developed. Besides, as in the pinched cylinder example, we can verify a proper representation of inextensional bending and, additionally, this is an excellent test for the ability of the element to model rigid-body motions.

Due to symmetry of the problem, only one octant of the shell is discretized with uniform meshes of proposed elements (Figure 8). Table 2 lists results of the convergence study through normalized midsurface displacements at points A and C. The displacements are normalized with respect to the values [6] $-u_y^{\mathrm{M}}(A) = u_x^{\mathrm{M}}(B) = 0.1013$ and $u_y^{\mathrm{M}}(C) = -u_x^{\mathrm{M}}(D) = 0.09785$, where u_x^{M} and u_y^{M} denote displacements of the midsurface in x and y directions. One can observe that developed schemes of analytical integration perform very well.

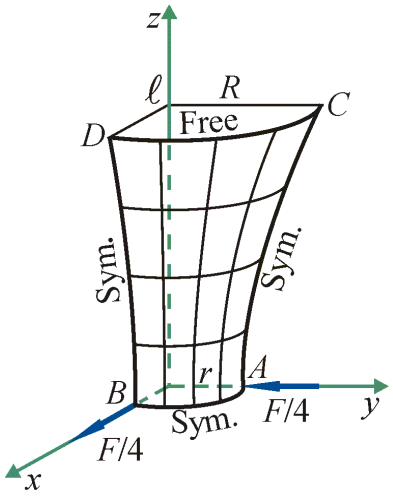

Figure 8: Pinched three-layer cross-ply hyperbolic shell with ply orientation [90/0/90], where $r=7.5$, $R=15$, $\ell=20$, $h=0.04$, $E_{\mathrm{L}}=4\times10^{7}$, $E_T=10^{6}$, $G_{\mathrm{LT}}=G_{\mathrm{TT}}=6\times10^{5}$, $\nu_{\mathrm{LT}}=\nu_{\mathrm{TT}}=0.25$, $F=4$

Mesh	EG6P4 [6]		EG9P4	
	$u_y^{\mathrm{M}}(A)$	$u_y^{\mathrm{M}}(C)$	$u_y^{\mathrm{M}}(A)$	$u_y^{\mathrm{M}}(C)$
2x2	0.5961	1.1474	0.6811	1.3119
4x4	0.8726	1.0337	0.8808	1.0221
8x8	0.9610	1.0089	0.9611	1.0087
16x16	0.9877	1.0021	0.9879	1.0022

Table 2: Normalized displacements at points A and C of the pinched three-layer cross-ply hyperbolic shell

6.2 Geometrically Non-Linear Examples

6.2.1 Pinched Hemispherical Shell

To investigate the capability of the proposed exact geometry shell element to model the inextensional bending and large rigid-body motions, we consider one of the most demanding non-linear tests. A hemispherical shell with 18^{o} hole at the top is loaded by two pairs of opposite forces on the equator. The geometrical and material data of the problem are shown in Figure 9.

Owing to symmetry, only one quarter of the shell is modeled with regular meshes of EG9P4 elements. Figure 10 presents load-displacement curves compared with those derived by the 16×16 mesh of S4R elements of Abaqus® [9]. It is seen that all results agree closely but the EG9P4 element is less expensive owing to the economical derivation of its tangent stiffness matrix.

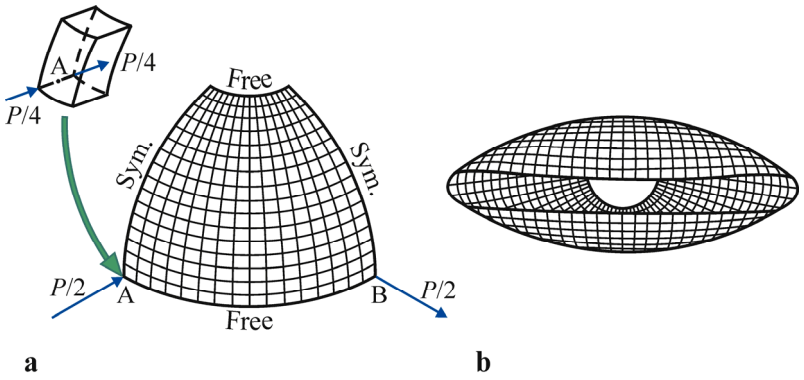

Figure 9: Pinched hemispherical shell: (a) geometry and (b) deformed configuration (modeled by 16×16 mesh), where $R=10,\ h=0.04,\ E=6.825\times10^7,\ \nu=0.3, P=100f,\ f=4$

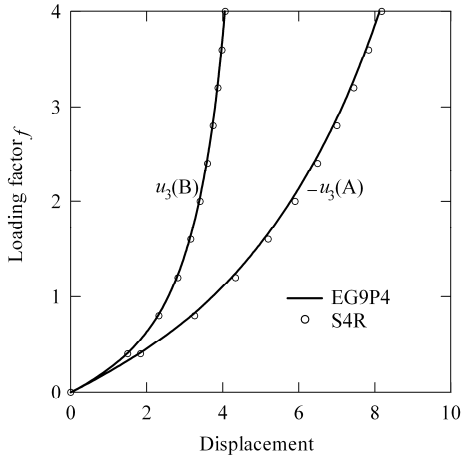

Figure 10: Midsurface displacements of the pinched hemispherical shell (modeled by 16×16 mesh)

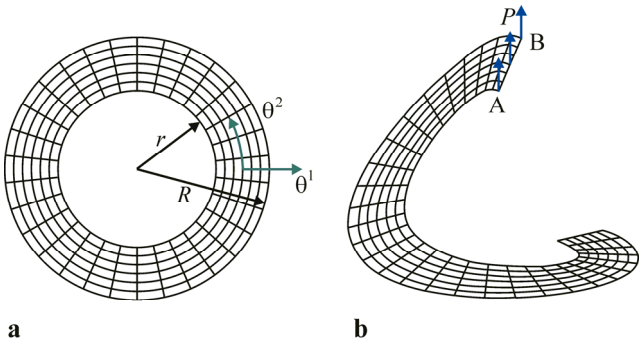

Figure 11: Slit ring plate under a line load: (a) geometry and (b) deformed configuration (modeled by 6×30 mesh), where $r=6,\ R=10,\ h=0.03,\ E=2.1\times10^7,\ \nu=0,\ P=0.8$

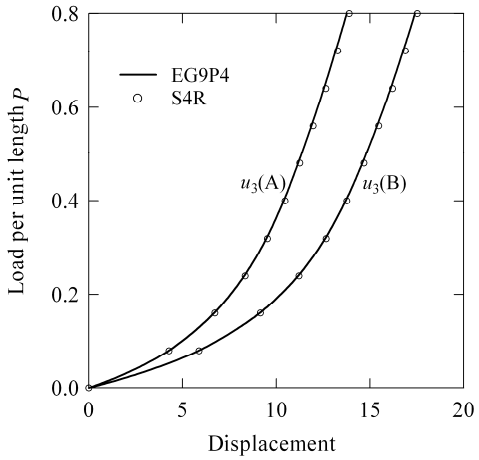

Figure 12: Midplane displacements of the slit ring plate (modeled by 10×80 mesh)

6.2.2 Slit Ring Plate under Line Load

This example is considered in the literature to test non-linear finite element formulations for thin-walled shell structures and has been extensively used by many investigators. The ring plate is subjected to a line load P applied at its free edge of the slit, while the other edge is fully clamped (Figure 11). The plate is modeled by a shell of revolution with geometrical parameters

$$A_1 = 1, \quad A_2 = r + \theta^1, \quad k_1 = k_2 = 0, \quad \theta^1 \in [0,\, R - r], \quad \theta^2 \in [0,\, 2\pi].$$

The displacements at points A and B of the plate, presented in Figure 12, have been found employing the uniform 10×80 mesh of EG9P4 elements. A comparison with Abaqus® S4R element [9] is also given.

7 Conclusions

The simple and efficient exact geometry assumed stress-strain four-node solid-shell element EG9P4 has been developed for analyses of homogeneous and multilayered composite shells undergoing finite rotations. The finite element formulation is based on the non-linear strain-displacement relationships, which are invariant under arbitrarily large rigid-body shell motions in a convected curvilinear coordinate system. This is due to our approach in which the displacement vectors of outer and middle surfaces are introduced and resolved in the reference surface frame. The proposed exact geometry solid-shell element model is free of assumptions of small displacements, small rotations and small loading steps because it is based on the objective fully non-linear strain-displacement relationships. This model is robust because it permits to use the complete 3D constitutive equations and coarse mesh configurations. The tangent stiffness matrix developed does not require expensive numerical matrix inversions that is unusual for the isoparametric hybrid/mixed shell element formulations and it is evaluated by using the 3D analytical integration.

Acknowledgements

The support of this work by Russian Foundation for Basic Research under Grant No 08-01-00373 and Russian Ministry of Education and Science under Grant No 2.1.1/660 is gratefully acknowledged.

Reference

[1] H. Parisch, "A continuum-based shell theory for non-linear applications", International Journal for Numerical Methods in Engineering, 38, 1855-1883, 1995

[2] G.M. Kulikov, S.V. Plotnikova, "Finite rotation geometrically exact four-node solid-shell element with seven displacement degrees of freedom", Computer Modeling in Engineering & Sciences, 28, 15-38, 2008.

[3] G.M. Kulikov, S.V. Plotnikova, "Non-linear strain-displacement equations exactly representing large rigid-body motions. Part I. Timoshenko-Mindlin shell theory", Computer Methods in Applied Mechanics and Engineering, 192, 851-875, 2003.

[4] G.M. Kulikov, S.V. Plotnikova, "Non-linear geometrically exact assumed stress-strain four-node solid-shell element with high coarse-mesh accuracy" Finite Elements in Analysis and Design, 43, 425-443, 2007.

[5] G.M. Kulikov, E. Carrera, "Finite rotation higher-order shell models and rigid-body motions", International Journal of Solids and Structures, 45, 3153-3172, 2008.

[6] G.M. Kulikov, S.V. Plotnikova, "Geometrically exact assumed stress-strain multilayered solid-shell elements based on the 3D analytical integration", Computers & Structures, 84, 1275-1287, 2006.

[7] B.F. Vlasov, "On the bending of rectangular thick plate", Transactions of Moscow State University, 2, 25-31, 1957 (in Russian).

[8] N.J. Pagano, "Exact solutions for rectangular bidirectional composites and sandwich plates", Journal of Composite Materials, 4, 20-34, 1970.

[9] K.Y. Sze, X.H. Liu, S.H. Lo, "Popular benchmark problems for geometric nonlinear analysis of shells", Finite Elements in Analysis and Design, 40, 1551-1569, 2004.